Research on Engineering Structures & Materials
www.jresm.org

Research Article

Green syntheses and characterization of Phragmites australis nanofibers on sustainable concrete

Fahad Saadi Almani [*,1, a], Farhad M. Othman [2,b], Alaa A. Abdul-Hameed [2,c]

[1]*Directorate of Water Resources in Karbala, Ministry of Water Resources, Karbala, Iraq*
[2]*Materials Engineering College, University of Technology – Iraq, Baghdad, Iraq*

Article Info

Article History:

Received 12 Oct 2025
Accepted 27 Dec 2025

Keywords:

Phragmites australis
Nano-fiber,
Cellulose,
Concrete,
Alkali treatment,
Compressive strength,
Flexural strength,
Sustainability and west plant

Abstract

Concrete suffers from low tensile capacity, high brittleness, and increasing environmental impact due to cement production. This study presents a green synthesis route for extracting cellulose nanofibers from Phragmites australis, an abundant invasive plant, and evaluates their effectiveness as a sustainable reinforcement for concrete. The novelty of the work lies in converting an environmental waste material into nano-cellulose fibers through an eco-friendly alkali-based extraction process, followed by mechanical milling to achieve nano-scale sizes (80–100 nm). The nanofibers exhibited increased crystallinity, enhanced purity, and improved surface morphology as confirmed by XRD, FTIR, SEM, XRF, and particle size analysis. Concrete mixes incorporating 5%, 10%, and 15% nanofibers were tested at 7, 28, and 90 days. The optimum performance occurred at 10% nanofiber content, which improved flexural strength by 36% (from 4.09 to 5.57 MPa) and maintained compressive strength at 29.4 MPa compared with the control (28.2 MPa). Physical properties also improved, with reductions in porosity and water absorption at the optimum dosage. However, 15% fiber addition caused strength and workability reductions due to fiber agglomeration and increased voids. These findings demonstrate that Phragmites australis nanofibers can serve as a low-cost and sustainable reinforcement to enhance concrete performance while valorizing an invasive plant. The study supports the broader trend of integrating bio-based nanomaterials into construction materials to reduce environmental impact and improve mechanical efficiency.

1. Introduction

Concrete is a principal building material in the world, as well as one of the most widely consumed materials after water [1]. But the materials are low in tensile strength, high in brittleness, weak in stress-strain capabilities and notoriously bad to produce given its carbon footprint. Green cement technologies, reactive powder concrete (RPC), low-emission materials, scattering fibers, and nanoparticles have been studied to avoid these limitations [2–6]. Nanoparticles smaller than 500 nm improve micro- and nanoscale hydration [6], increase the mechanical rigidity [7–10] and lead to higher electrical resistibility [11,12]. In the category of nanoparticles, cellulose (C) or CNFs obtained from the fibers extracted from plants have attracted significant prominence owing to their large surface area (100 m^2/g), high aspect ratio (100), high crystallinity, low density and strength [13]. They are based on CNF, a renewable and recyclable material with biodegradable properties. In terms of structural composition, CNFs are predominantly cellulose with lignin and hemicellulose—whereas the latter two provide structure, their amorphous nature renders them inferior to cellulose. Different types of plants including cassava bagasse [14], wheat straw [15], cotton [16], bamboo [17], and sugar palm [18] have been employed as the sources to produce CNFs. Green synthesis methods, especially ecofriendly alkali-

*Corresponding author: mae.20.30@grad.uotechnology.edu.iq
[a]orcid.org/ 0009-0006-4216-0370; [b]orcid.org/0000-0002-2289-5656; [c]orcid.org/0000-0003-4492-6369
DOI: http://dx.doi.org/10.17515/resm2026-1243ic1012rs

mediated extraction routes, not only eliminate toxic substances and lower energy requirement when compared with the traditional acid hydrolysis method but also provide a means for producing f -MNCs that can address some issues in natural concrete materials such as poor strength and environment vulnerability. Despite the promise of CNFs in improving flexural behavior, crack resistance, and microstructural densification, most studies rely on commercial fibers or energy-intensive methods, which do not address cost, environmental impact, or availability in resource-limited regions. Phragmites australis (PA) is selected in this study due to its fast growth, invasiveness, and environmental burden; converting this abundant biomass into nanofibers provides dual benefits of ecological mitigation and a zero-cost, renewable raw material. PA fibers naturally possess low lignin content, fine morphology, and high aspect ratio, making them highly suitable for nanofiber production, while also stabilizing cement-based products by reducing chemical, autogenous, and drying shrinkage, and being heat-resistant [19,20]. This research introduces a green, alkali-based nano-extraction method combined with high-efficiency planetary ball milling to produce nanofibers with particle sizes of 80–100 nm, improved crystallinity, and enhanced surface roughness, representing a novel contribution to sustainable nanofiber production from invasive plants. Unlike previous studies that focused on commercial or agricultural fibers, this work employs a fully green extraction technique, provides comprehensive multi-scale characterization (XRD, FTIR, SEM, XRF, particle size analysis), and evaluates the mechanical and physical performance of concrete reinforced with nanofibers at 5%, 10%, and 15%, including regression analysis and optimal-dose identification. The overall aim is the preparation and characterization of cellulose nanofibers from Phragmites australis and their effects on the mechanical and physical properties and confirmed that these types of nanofibers can improved strength, reduced porosity and bring a negligible Change in the unit weight of hardened paste. durable, cheap reinforcement based on new construction and as well as a response to the modern age requirements. environmental obstacles induced by PA overproduction.

2. Materials and Methods

2.1. Materials

The experimental work is divided into two parts: the part one deals fiber preparation and its characterizations, while the second stage consists of preparation and performance, respectively.

2.1.1 Preparation of Nano-Fiber

In the present work plant fibers were obtained from waste phragmites australis in the search for generation of sustainability in concrete. Extraction of Phragmites australis fiber from the Northern Karbala Drain. The fibers were washed thoroughly with distilled water to remove any surface impurities and air-dried at room temperature. Sodium hydroxide (NaOH) was purchased from SDFCL (Scientific Laboratory Supplies) sourced from Areej Al-Forat Office for engineering and chemical supplies, Baghdad, Iraq.}, and as an alkali treatment to improve the surface properties of the fibers. This choice of materials based on locally available plant waste and resources, conforms to the concept of sustainable building by maintaining the mechanical integrity of fabricated composites.

2.1.2 Preparation of Chopped Fibers

The Phragmites australis Wastes The wastes of Phragmites australis [as shown in Figure 1(a) were collected, washed well and then cut into (10-15) cm length in Figure 1(b). They were then water-retted for a period of 24 hours to eliminate impurities and waxy contents. They were then 24 hours to dry in the air before they can be treated chemically (alkali).

(a) (b) (c) (d)

(e) (f) (g) (h)

Fig. 1. (a) Materials (b) Cutting & Washing. (c) alkali treatment by 4% NaOH. (d) Washing with distilled water (neutralization). (e), (f) Drying Process. (g) Blender process (h) Milling Process

2.1.3 Treatment of Chopped Fibers

Sodium hydroxide (NaOH) is applied here to fibers which create water with the alkali-sensitive hydroxyls (OH), lowering the moisture absorption tendency. This is believed to solubilize some hemicellulose, lignin, pectin and waxy layer by which increasing surface adhesion (rougher topography), mechanical interlocking and removing impurities [21-23]. Alkali treatment disrupts hydrogen bonds, enhances thermodynamic stability, eliminates microdata and decreases fiber diameter leading to improved aspect ratio and effective surface area [25, 26]. For the fibers to be utilized in composite materials, the plants were first treated with 4% NaOH solution at 100°C for 2 h [27,28] (Figure 1(c)), followed by rinsing with distilled water (neutralization) as presented in Figure 1(d), and then were dried at 60°C during up for overnight hours presented in Figure 1(e, f). 4% NaOH concentration, 100°C treatment temperature and 2 h treatment time were chosen with reference to literatures, also with consideration of the material itself. Prior studies on natural fibers such as sisal, banana, and Phragmites-based composites reported that NaOH concentrations between 2–6% effectively remove hemicellulose, surface waxes, and amorphous lignin without degrading cellulose structure. Similarly, a treatment temperature of 100°C accelerates alkaline penetration and improves the removal of amorphous components, while the 2-hour duration ensures complete chemical reaction without causing fiber over-degradation.

2.1.4 Blender and Milling

The dried material was ground using a blender and sieved through a 0.1 mm sieve to obtain uniform fiber size. The sieved fibers were then subjected to Planetary Ball Mill (Model: XQM-0.4A) for 4 hours at 550 rpm with balls of varying sizes placed in the device, weighing ten times the weight of the fibers. to achieve Nano-scale dimensions according to ISO/TS 20477:2017, as shown in Figure (1) (g, h).

2.2 Inspection of Nano-Fibers

The are several techniques can be used to inspect texture of materials such as:

2.2.1 X-Ray Diffraction (XRD)

The XRD patterns of nano-fiber samples were measured using Japan's XRD-6000 at the Nanotechnology and Advanced Materials Centre of the University of Technology. The measurements were taken from

10-60°(2θ) using a scanning rate of 2°/min and 0.02° step size. Equation (1) was used to compute the cellulose crystallinity index (CrI) [29].

$$CrI\ (\%) = (1 - Iam / Imax) \times 100 \quad (1)$$

Where Imax is the equivalent intensity of the maximum peak and Iam is the intensity of the amorphous fraction. For the calculation of the CS, the method used was established by Scherer's relations as expressed by the equation below:

$$CS = K\lambda / \beta \cos \theta \quad (2)$$

where K is the constant (0.89); λ corresponds to the intensity of radiation; β denotes the full-width at half-maximum (FWHM); and θ is the Bragg's angle[30].

2.2.2 The Scanning Electron Microscopy

SEM analysis was conducted using the VEGA TESCAN SEM instrument, with an accelerating voltage of 20.00 kV. The examination was performed at the Ministry of Industry and Minerals, Industrial Research and Development Authority.

2.2.3 Measuring Particle Size

American (Brook Haven 90 Plus) (5.0-5000.0) nm particles were tested for size at the University of Technology's Nanotechnology and Advanced Materials Centre.

2.2.4 FTIR Analysis

FTIR were done in a FTIR spectrum made in Germany, with 4000 to 400 cm−1 as the wave number and 0.9 cm−1, it used to identify the chemical analysis of materials in their various states by detecting the chemical bonds present in the material.

2.2.5 X-Ray Fluorescence

The nanofiber analysis was conducted using an X-Ray Fluorescence (XRF) instrument, model Spectro Xepos, manufactured in Germany by Ametek was carried out in Iran. This advanced device is renowned for its high precision in chemical element analysis through X-ray fluorescence technology.

2.3 Concrete Mix Design

For the concrete matrix, LAFARGE The major binder utilized was ordinary Portland cement (OPC). Fine aggregates (sand) and coarse aggregates (gravel) were sourced from the Karbala quarries and were pre-tested to confirm compliance with laboratory specifications for grading, cleanliness, and strength. All mixing and curing were performed using potable water. The 1:2:3 proportion of cement, sand and gravels by weight were adopted as concrete mix design based on ACI standard. The influence of fiber content addition in the mechanical and durability properties was evaluated by adding plant nanofibers at 5%, 10% and 15% w/w cement. The (ACI) was maintained at 0.5 to attain sufficient workability and an optimal compressive strength. This procedure guaranteed a homogeneous and reproducible blended mixture capable of efficiently realizing the reinforcing potential, in terms of hardness, of the plant nanofibers by maintaining the required performances level.

2.4 Sample Preparation

Firstly, all raw materials (cement, sand, gravel and plant fiber) were weighed according to the design mixture ratio of 1:2:3 (cement: sand: gravel) by weight, with plant nanofibers added at 5%, 10%, and 15% of cement weight Table 1 presents the mixing ratios and prepared samples, where Phragmites australis fibers are represented by (ANF%). The mixing process was carried out using a flat type mechanical mixer to ensure homogeneous dispersion of fibers. First, the tested cement is as shown in the table 3 was mixed with fibers and then with dry ingredients (sand and gravel) which physical examination are shown in Table 2 for 60 seconds at low speed to achieve a uniform mixture. A specified amount of water was added until the target workability was reached. After mixing, fresh concrete was poured into cubic molds (100×100×100 mm) for compressive strength tests and prismatic molds (75×75×300 mm) for flexural (flexural) tests. The samples were covered and dried at room temperature (about 20-25°C) for 24. The demolded specimens were moved to a curing tank in which

potable water was added and kept for all subsequent periods of 7, 28, 90 days in order to ensure full filling of hydration capacity and development of strength. Compressive and bending strength tests were subsequently carried out for the cubic samples and prismatic samples, respectively, under a universal testing machine (at 7 days, 28 days and 90 days). These methods guaranteed homogeneous specimen preparation and yielded reliable data for comparing the mechanical behavior of FRC specimens with that of non-reinforced (standard) ones.

Table 1. Mix proportions and prepared samples

Specimen	Cement%	Quartz sand, %	Gravel, %	ANF, %
Control	100	100	100	
CANF1	95	100	100	5
CANF2	90	100	100	10
CANF3	85	100	100	15

Table 2. Properties of sand and gravel

Physical Properties	FA	CA	B.S limits 12620
Specific gravity	2.57	2.6	-
Dry compacted density (mg/m3)	1.8	1.9	-
Water Absorption (%)	0.82	1.7	-
SO3 (%)	0.113	0.054	≤ 0.2
Fineness modulus	3.4	0.05	-

Table 3. Chemical composition and main compounds of cement

Oxid and Composition	CaO	SiO_2	Al_2O_3	Fe_2O_3	MgO	SO_3	L.O. I	Insoluble	Free Lime	C_3S	C_2S	C_3A
% Content	59.89	19.8	6.1	3.32	1.64 ± 0.005	2.30 ± 0.03	3.70 ± 0.01	0.65 ± 0.005	0.81	42.02	26.7	2.44
B.S 4027 Limits	-	-	-	<5	<2.5	<4	<1.5	-	-	-	-	-

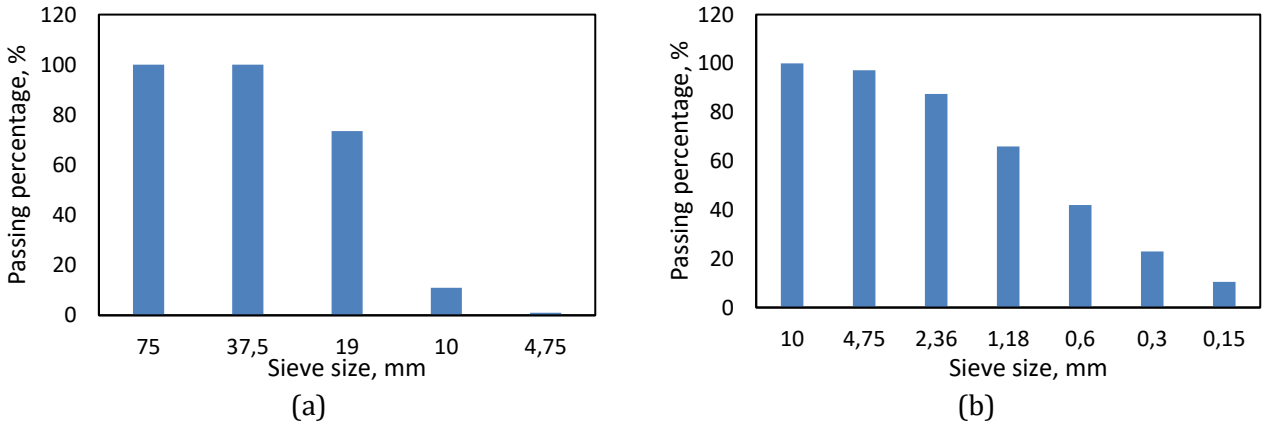

Fig. 2. Physical characteristics of (a)Sand (FA) and (b) Gravel (CA)

The fiber dosages of 5%, 10%, and 15% by weight of cement were chosen based on two considerations:

- Benchmarking from literature, where most natural-fiber-reinforced concretes exhibit optimal mechanical performance within 1–15% addition (depending on fiber size and processing). Studies on nano-cellulose from palm, cassava, and bamboo reported diminishing strength at dosages above 15% due to balling effects and increased porosity.

- Avoiding excessive loss in workability, since preliminary trial mixes in this study showed that fiber contents exceeding 15% significantly reduced slump and caused fiber agglomeration even with extended mixing.

2.5 Inspections of Fabricated Concrete Samples

The following tests are conducted on concrete specimens.

2.5.1 Fresh Concrete Workability Test

To analyze the impact of nano-fiber on concrete workability, all concrete mixes had constant water-to-cement ratio (W/C). As stated in BS1881-102 1983 [31], slump testing is performed using a cone (300×100×200) mm (height, top diameter and base diameter) to measure the influence.

2.5.2 Physical Properties Test

Dry density, porosity and water absorption tests were performed in accordance with ASTM C642-97. The test was performed on portions of concrete samples previously hydraulically compressed. Samples were oven dried for determining initial dry mass (w1). The samples were then immersed in water for 24 h to reach saturation, followed by solvent removal from surface. The mass surface-dry saturations (w2) were then measured after immersion. Finally, the samples were completely submerged in a beaker filled with water and weighed to obtain the apparent immersed mass (w3). using the following formula [32].

$$Dry\ density\ (g/cm^3) = [w1/(w2 - w3)] \times \rho w \quad (3)$$

$$Absorption\ of\ Water = [(w2 - w1)/w1] \times 100\ \% \quad (4)$$

$$Porosity = [(w2 - w1)/(w2 - w3)] \times 100\% \quad (5)$$

Where $w1$: the dry specimen's weight (g), $w2$: the wet specimen's weight (g), $w3$: the submerged specimen's weight in water (g), and ρw: the density of water, which is (1 g/cm3).

2.5.3 Compressive Strength Test

Compressive strength tests were conducted. Each test was performed on three specimens (n = 3), and average values are reported. Statistical significance between mixes was confirmed using one-way ANOVA ($p < 0.05$). with the method defined in B.S.1881-116. The test was performed using a compressive strength testing device (TONI PACT 3000/Germany). The upload speed was roughly 0.25 megapascals a second. The compressive strength of three 100×100×100 mm concrete samples (average) was calculated for each mixture. The exam was performed 7, 28, and 90 days after preparation. Calculating compressive strength using the stated relationship [33].

$$\sigma = P/A \quad (6)$$

Where σ: compressive strength, (MPa); P: ultimate compressive load, (N); A: area of the sample, (mm^2).

2.5.4 Flexural Strength Test

BS 12390-5: 2009 (the bending test), in this experiment a prismatic mold with dimensions (75×75×300) mm was used. A three-point flexural strength test is performed to generate the crack. A speed of 0.04 mm/min was applied. The results were recorded for cast and cured concrete specimens after 7, 28, and 90 days. The following law [34] was used to obtain the flexural strength.

$$Fct = F \times I/(d1 \times (d2)^2 \quad (7)$$

Replaceable with: Fct: Flexural strength, MPa (N/mm^2); F: Maximum load, N; I: Distance between supporting rollers, mm. lateral dimensions of the specimen in mm; d1 and d2.

3. Results and Discussion

3.1 XRD Results

The XRD analysis for the chemically treated Phragmites australis fibers demonstrates distinct diffraction peaks corresponding to the crystalline structure of cellulose I, enhanced by sodium hydroxide (NaOH) treatment, which effectively removed non-cellulosic components such as lignin and hemicellulose. The primary peaks associated with cellulose Iβ appear at 2θ ≈ 14.902°, 16.494°, 22.842° (strongest peak), and 34.882°, aligning with JCPDS card no. 03-0289, confirming that the crystalline structure of cellulose is preserved [35] Figure 3(a). silicon oxide (SiO2) characteristic's at 2θ ≈ 26.479°, 50.583° and by far the strongest peak is observed at 26.479° which matches with JCPDS74–204411 card no:461441. This is due to the presence of residual silica, which derives from the inherent plant fibers. Moreover, Al peaks for aluminum oxides (Al2O3) were also observed at 2θ ≈ 32.802°, 45.642° and the highest intensity peak at 67.245° in compliance with JCPDS card no.:461131. This indicates the existence of alumina, probably caused by minerals contents in the fiber matrix. In addition, calcium oxide (CaO) was recognized by XRD peaks at 2θ ≈ 37.346° and 53.854° (JCPDS card no. etz371497), which is due to the presence of calcium-containing compounds that might improve compatibility between the fibers and cementitious materials. These results revealed that the alkali treatment enhanced the crystallite structure of cellulose, while retaining beneficial inorganic phases such as SiO2, Al2O3, and CaO. The presence of those mineral admixtures could offer an effective profit to polymeric strength and log-time durability of cementitious mixtures [36,37].

The responses in the XRD patterns of the treated Phragmites australis nanofibers show a cellulose Iβ diffraction peak at 2θ ≈ 14.9°, 16.4°, 22.8° and 34.8°. The strongest peak in the 22.8° is ascribed to the crystalline cellulose regions. The CrI increased significantly, in the Segal's approach, from ⍰46% of raw fibers (let us note that this assumes average values of polyanionic ones reported in literature) to 72% for treated nanofibers. This enhancement indicates the efficient extraction of amorphous hemicellulose and lignin.

A slight peak sharpening and reduction in FWHM indicates an increase in crystallite size, attributable to the elimination of amorphous content and exposure of more ordered cellulose domains. This enhancement in crystallinity is desirable, as higher CrI improves thermal stability and contributes to better interfacial bonding with cement hydration products.

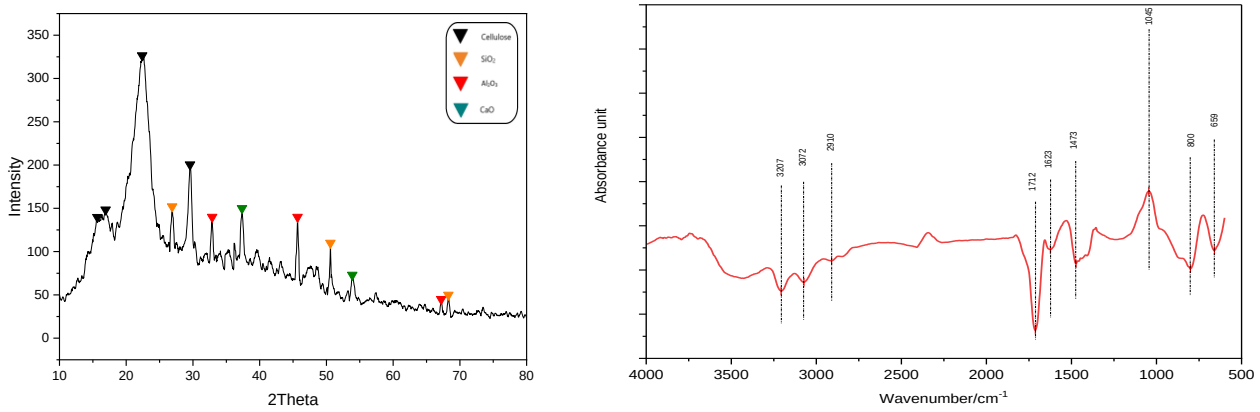

(a) (b)

Fig. 3. (a) XRD result (b) FTIR result

3.2 FTIR results

FTIR spectra of cellulose fibers derived from Phragmites australis show distinctive structural and chemical features that attest its chemical treatment process in the domain of shown in Figure 3(b), a broad absorption band around 3300–3000 cm^{-1} were attributed to hydroxyl (O-H) stretching vibrations which confirms the presence of cellulose [38]. The significant abundance of this band at Phragmites australis is indicative of a high concentration of cellulose and strong hydrogen bonding. Absorption bands at 2800–2900 cm^{-1} in which attributed to aliphatic C-H stretching, confirming the

existence of cellulose and little amounts of hemicellulose residues [38]. A striking feature of the carbonyl (C=O) stretching region at approximately 1730 cm^{-1} is the marked decrease of this peak in Phragmites australis, indicating the efficient elimination of residual hemicellulose and lignin [39], while the clean peaks in the fingerprint region (1000–1200 cm^{-1}) of the Phragmites australis spectrum imply high crystallinity and cellulose purity. The chemical treatment was most efficient in the elimination of non-cellulosic components (lignin and hemicellulose) from Phragmites australis leading to better structural integrity of fibers. Thus, Phragmites australis based fibers do possess potential for application in concrete, especially related to mechanical properties enhancement (i.e. compressive and tensile strength). FTIR spectra displayed prominent changes from lignocellulosic transitions:

- 3300–3000 cm^{-1} (O–H stretching) band was increased in relative intensity, indicating the stronger hydrogen bond which was generally typical for a purified cellulose.
- The C–H stretching peaks at 2800–2900 cm^{-1} were reserved, indicating the backbone of cellulose maintained.
- The carbonyl absorption at 1730 cm^{-1}— attributed usually to hemicellulose—was greatly reduced, reflecting the elimination of this compound.
- The bands around 1240-1270 cm^{-1} (lignin aromatic groups) also decreased significantly.
- The inherent region (1000–1200 cm^{-1}) proved more defined, indicating a higher degree of crystallinity as confirmed with XRD.

In combination, XRD and FTIR make it clear that the green alkali treatment effectively removes non-cellulosic components from the fibers and improves the order in their structure which is required for effective reinforcement of cementitious composites

3.3 Particle Size Analysis

The Phragmites australis fibers exhibited a moderately uniform particle size distribution and a greater aspect ratio, as shown in Figure 4. Average particle size was between 45–100 nm indicating nano-scale dimensions of the results. Hence, the alkali treatment and ball-milling were effective methods to reach nano scale fiber size, contributing to better bonding between the fiber and the matrix as well as better mechanical properties of composites. One point to notice is the aspect ratio of Phragmites australis fibers that is very high, showing super reinforcement potential. This behavior is explained by the lower lignin content and finer natural morphology of Phragmites australis. A further reason for the loss of structural security through Phragmites australis fibers is attributed to lignin, as a highly cross-linked co-polymer that enhances structural stability and mechanical strength which becomes compromised due to its poor presence in Phragmites australis fibers, which allow for mechanical disintegration to occur more frequently rendering smaller this nano-scale particle considerably in a more homogenous spectrum. The moderate PDI values of Phragmites australis fibers also indicate a potential for better dispersion in the concrete matrix. In particular, these fibers are commonly beneficial in enhancing the performance of cementitious composites due to their uniform and fine geometry, resulting in enhanced toughness, crack resistance, and mechanical properties.

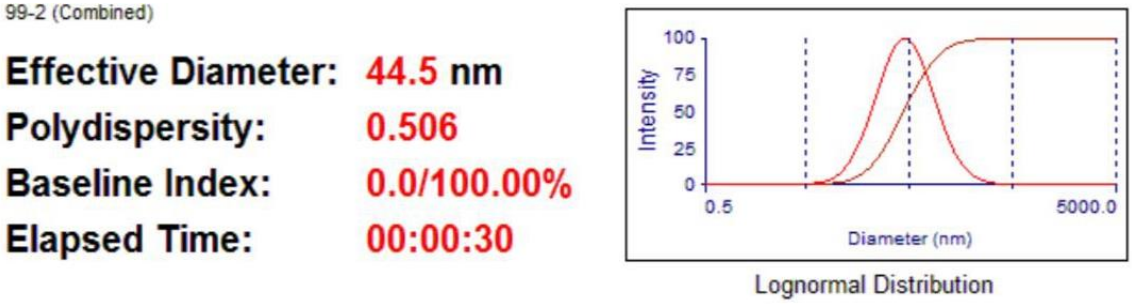

Fig. 4. Illustrates the PSM for Phragmites australis

3.4 SEM Result

The nano-fibers extracted from Phragmites australis also exhibits different morphological structures showing characteristics of nano-structure, which is an inherent feature of its capability as a possible reinforcement system in binders. The Figure (5)(a) shows entangled, fibrillated fiber bundles with a

highly irregular, rough surface that increases mechanical interlocking within a matrix. Fiber aspect ratio: This attribute specifies the proportion of the fiber's length to its diameter; high aspect ratios (length to diameter ratio) are desirable to enhance tensile strength and crack resistance. As seen in Figure (5)(b) taken at a higher image magnification, the individual fibers remain clearly separated from each other and possess a relatively uniform diameter on nanometer length scales consistent with effective mechanical processing and chemical treatment. Rugged and porous fiber surfaces provide higher specific surface area, which increases the bonding potential with cement hydrates when mixed. In addition, residue of impurities or residual lignin outside the fiber surfaces indicates that alkaline treatment is successful and cellulose purity is high. These microstructural features confirm that the prepared Phragmites australis nano-fibers possess the desired properties for reinforcement, contributing to improved mechanical performance when used in concrete composites.

Figure 5: Illustrates the SEM result of CANF: (a) Aggregated Structure and (b) Showing Surface Morphology. From the SEM images, adjourned membranes of fibrillated rough surface and nanofibers exhibiting a very heterogeneous (unsmooth) outer layer suggested favorable mechanical interlocking. Images obtained at high-magnification revealed fiber diameters of 80–120 nm, thus verifying the nanoscale size. The rough and porous texture increases the interface area and enhances bond with C–S–H gel. No significant surface damage was detected for any of the samples regardless of treatment, suggesting that no deterioration on the cellulose crystalline framework due to NaOH treatment and ball milling occurred. These morphological features account for the good stress transfer mechanism evidenced during mechanical tests, especially at 10% filler concentration.

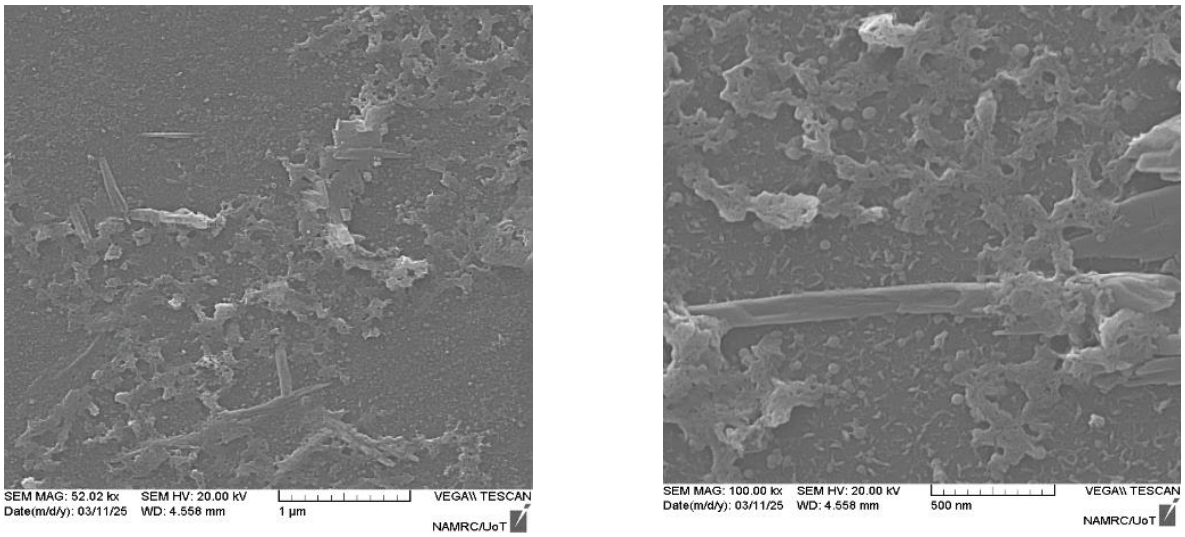

(a) (b)

Fig. 5. Illustrates the SEM result of CANF: (a) Aggregated Structure and (b) Showing Surface Morphology

3.5 XRF Result

The fibers of Phragmites Australis: The XRF analysis the results presented in this paper show key elemental and oxide composition that are responsible for the potential use of the tested fibers as concrete addition. These fibers show the silica (SiO_2) amount at 5.811% as displayed in table (4), and would indicate high pozzolanic activity which will improve long-term strength, as well as durability of concrete [41]. Furthermore, the aluminum oxide (Al_2O_3) content is 1.883% showing a high potential in producing calcium aluminate hydrates which will be beneficial to enhancing the durability and chemical resistance of concrete structures [40]. Iron oxide (Fe2O3) at a content of 0.3714% has minor pozzolanic significance and could also affect the coloration of concrete product [41]. fibers, have high amount of carbon (88.76%\uff08) And they may increase thermal insulating properties on concrete too [42]. High SiO2 and Al2O3 contents in the Phragmites australis fibers mean they are well-qualified for enhancing the long-term durability of concrete, which have advantages such as pozzolanic reactivity, enhanced chemical resistance and maintenance of mechanical strength over time.

Table 4. Result of XRF for Phragmites australis

Element/ Oxide	MgO	Al_2O_3	SiO_2	P_2O_5	SO_3	K_2O	CaO	MnO	Fe_2O_3	ZnO	Other element and oxide	C
Concentration (%)	0.28	1.88	5.81	0.47	0.36	0.23	1.33	0.02	0.37	0.02	0.43	88.76

3.6 Slump Test Findings

Slump test results in Fig. 6 represent the reduction of concrete workability (except for 5 % fiber) by adding Phragmites australis fibers to it when comparing with plain concretes. The lowest/highest slump is obtained for the plain concrete (7 cm) and can be considered to have good workability. The findings shows when Phragmites australis. The slump value decreased by 14.3% at 5% fibers (6 cm), 31.4 % for 10% fibers (4.8 cm) and decrement of optimum point was found to be about47.1 (&) at 15% fibers presence, implying that workability decreases proportionally with increase in fiber content. The low slump reduction is explained by the nanometer-size of the fibers, allowing them to be more homogeneously dispersed in the cement-based matrix. In order to solve this problem, the application of superplasticizer or water-reducing agent is proposed as a potential approach for enhancing the workability without harming mechanical properties. This reduces the friction and fritting effect, which is usually more significant when it co-works with larger fiber reinforcement [43]. According to relevant standards, such as ASTM C143, the slump value typically ranges from 100 mm to 35 mm, depending on the intended use of the concrete structure. For general construction, a slump value between 75 mm and 100 mm is considered ideal for maintaining workability and cohesion. for roads, it is around 35 mm; and for concrete works, it ranges from 50 mm to 60 mm. The results indicate that Phragmites australis nanofibers present a compromise between processability and mechanical reinforcement. The fact that they achieve adequate slump values, their fiber-matrix interaction is enhanced, and both mechanical performance and workability can be engineered simultaneously, indicates their role in advancement of construction [44].

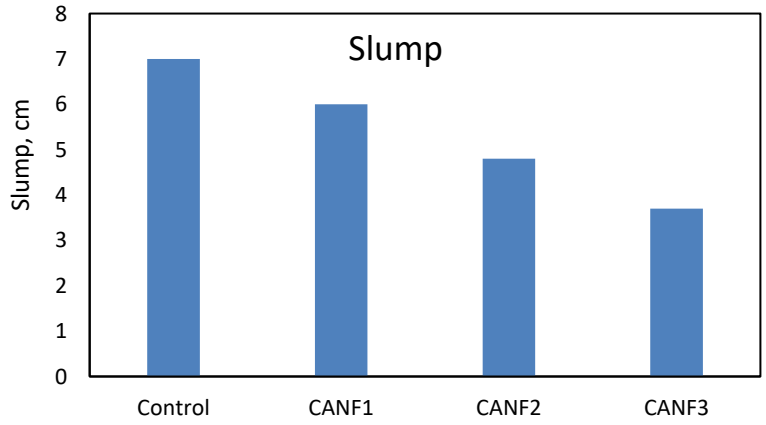

Fig. 6. Slump test results

3.7 Physical Properties

Results of the physical properties evaluation of concrete with different percentages by weight of Phragmites australis nanofibers (CANF) (5%, 10%, and 15%) are illustrated in Figure (7). Control concrete presented the greatest water absorption and porosity, which was reduced when 10% CANF was added, obtaining the best performance. The decrease in water absorption was associated with a better densification of the matrix and a better fiber-matrix bonding, which both prevented water ingress and a formation of voids. At fiber contents of 15%, however, porosity and water absorption increased slightly, which may have been caused by fiber agglomeration and decreased compaction efficiency [45]. Moreover, dry density decreased progressively with increasing the CANF content due to the lightweight property of the fibers and the partial replacement of the denser cement material. From these outcomes, the addition of 10% CANF contributes to a more systematic improvement in physical characteristics by decreasing both porosity and water absorption but without an increase in

density making the concrete matrix more durable and has a finer quality [46]. The findings highlight the significance of proper curing in fiber-reinforced concrete performance, and indicate that chemical treatment of fibers should be further implemented for proper fiber-cement compatibility [47].

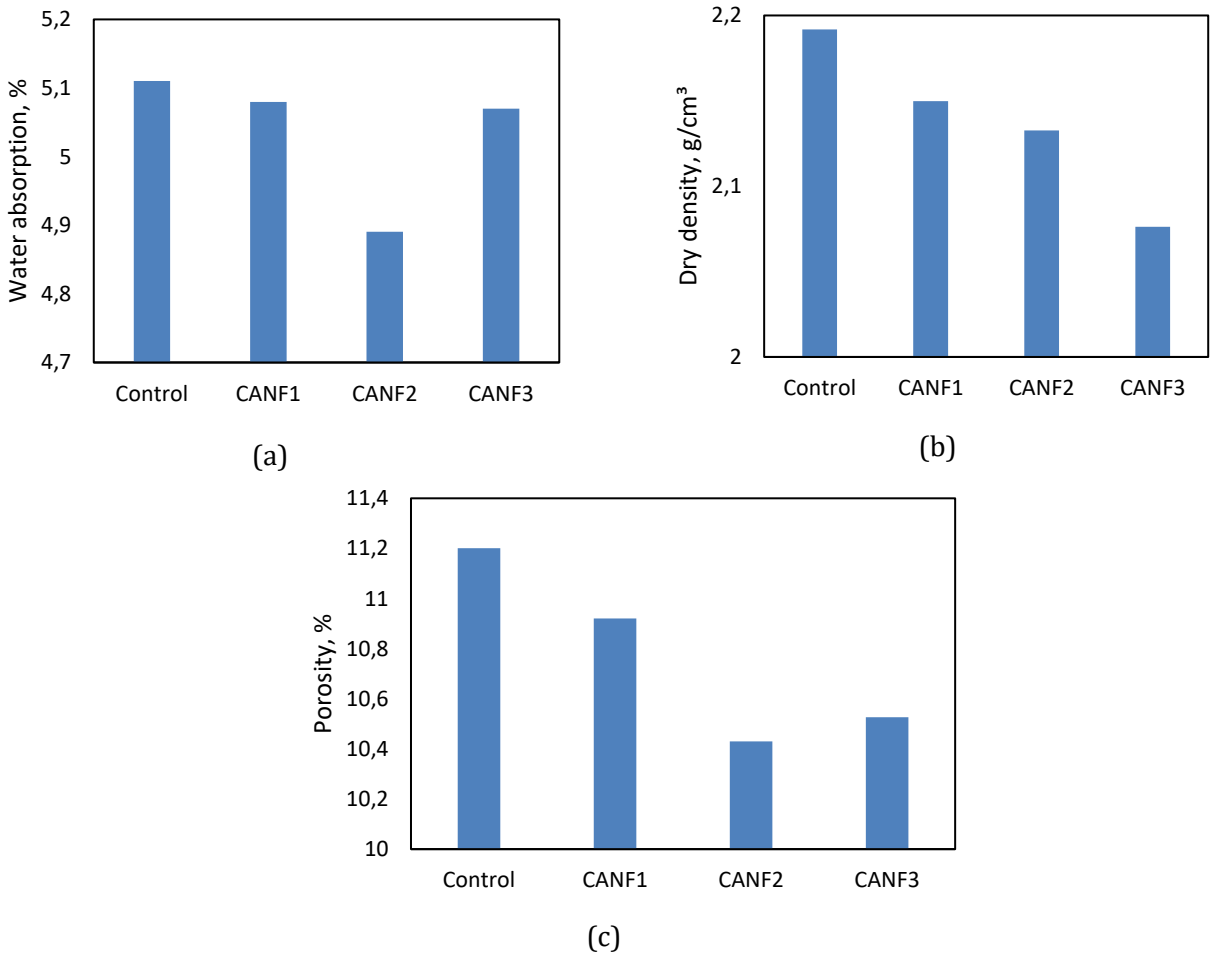

Fig. 7. Physical Results for concrete (a) Dry density (b) Water absorption (c) Porosity

3.8 Mechanical Inspection Results

Figure 8 shows mechanical performance of concrete composites reinforced with Phragmites australis nanofibers (CANF) by measuring compressive and flexural strength at (7, 28 and 90) days. Figure 9, table (5) illustrates the regression analysis for both flexural and compressive strengths. Both properties were enhanced with 5 and 10% CANF addition and depressed with the addition of 15% fiber. Fig.2 (d) indicates that the lowest compressive strength was observed in the control mix for all curing periods and TE stressing condition of 90 days, while maximum density achieved at which age induced best stature value (10% CANF mix). This difference may be attributable to either hydration or further densification improvements of matrix with progressing curing periods. The trend seen in flexural strength followed the same pattern, such as that for 10% CANF mix always it was higher than control and other fiber dosage further strengthening the maximization of flexural strength at 90 days. This increases interfacial strength due to fiber bridging mechanism, which tends to improve crack resistance and energy absorption. However, with the 15% CANF as contents increases porosity and the porosity of the green body would further agglomeration of fibers these could volume and if fiber–matrix bonding was not strong enough, compact decreased crack structures by weak fiber adhesion. As a result, fiber cohesions are predicted to partially fail during continuous sintering. It can be concluded from the results shown here that an addition of 10% fiber remains at the critical value when the synthesized MMCs possessed high-quality mechanical behavior and excessive incorporation led to performance degradation. It is also reported that natural fibers have the potential to increase life span of concrete composites as well as increasing toughness and durability but still prevents the use of construction materials from being non- environmentally friendly [46].

Table 5. Mechanical test results

Sample	Compression			Flexural		
	7 days	28 days	90 days	7 days	28 days	90 days
Control	21.7	25.3	28.2	3.13	3.79	4.09
CANF1	22.8	28.1	30.2	3.62	4.68	4.98
CANF2	21.9	27.5	29.4	3.98	4.8	5.1
CANF3	21.1	25.1	28.2	3.02	3.56	3.85

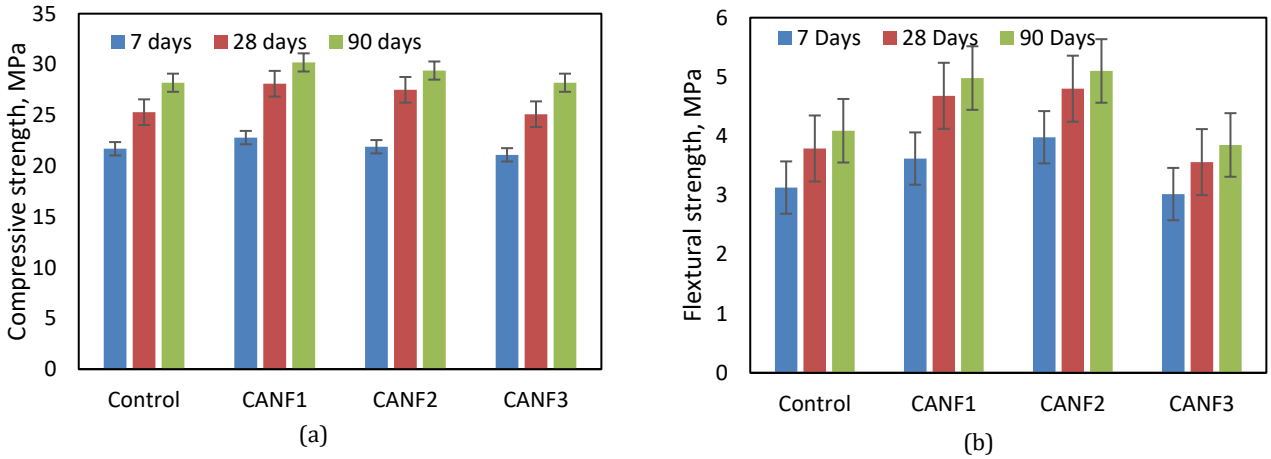

Fig. 8. (a) Compressive results and (b)Flexural results

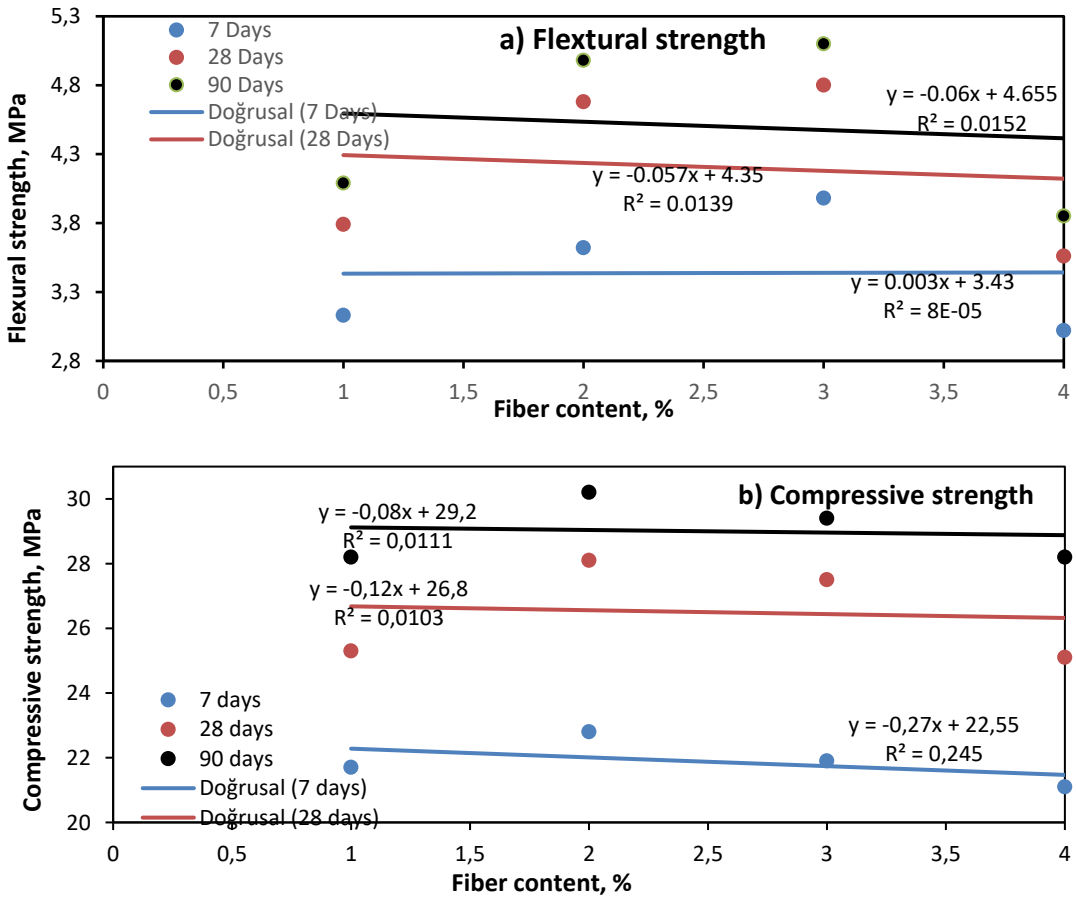

Fig. 9. Regression analysis (a) flexural strength (b) compressive strength

5. Conclusions

This work presents evidences that the Phragmites australis nanofiber (PANF) fabricated via a green alkali-extraction approach, possesses promising potential as an efficient reinforcement material for concrete. The addition of these nanofibers improved the mechanical and physical properties of concrete to a certain degree at the optimized mixing balance. In particular, with the incorporation of 5% fiber content, a gain in compressive strength by approximately 7% was reported, whereas flexural strength displayed the highest increase of around 36%, which was obtained at an addition of 10 % fiber. These improvements are attributed to the nanoscale fibrillar structure of the salt-treated fibers, which provide crack bridging, enhance fiber–cement interfacial bonding and also contribute towards a better matrix densification.

From a scientific aspect, the research offers new knowledge on how cellulose nanofiber from an invasive species interacts with cementitious materials. Enhanced crystallinity, surface-roughness and concentration of oxides (SiO_2, Al_2O_3, CaO) on extracted fibers contribute to changes in hydration processes, hence microstructural development. This study demonstrates an environmentally benign method for the conversion of abundant waste biomass into a value-added nanomaterial for greener construction industry.

From a practical point of view, the results show that P. australis nanofibers can be used to improve the flexural response of concrete when high resistance under bending is required, as in slabs, pavements or precast structural elements. Durability performance, in particular, resistance against freeze–thaw cycles, thermal stability, chemical attack and long-term shrinkage behavior need to be extended in future studies. Study of the hybrid fiber system and optimization of dispersion techniques can bring to even better mechanical properties for broader industrial application.

References

[1] Ndahirwa D, Zmamou H, Lenormand H, Leblanc N. The role of supplementary cementitious materials in hydration, durability and shrinkage of cement-based materials, their environmental and economic benefits: A review. Cleaner Materials. 2022 Sep 1; 5:100123.

[2] Kene KS, Vairagade VS, Sathawane S. Experimental study on behavior of steel and glass fiber reinforced concrete composites. Bonfring international journal of industrial engineering and management science. 2012 Dec 1;2(4):125.

[3] Dahesh AZ, Othman FM, Abdulhamead AA. Influence of Microfibers Additive on the Selfhealing Performance of Mass Concrete. Engineering and Technology Journal. 2021;39(01):104-15. https://doi.org/10.30684/etj.v39i1A.1581

[4] Salavati-Niasari M. Nanodimensional microreactor-encapsulation of 18-membered decaaza macrocycle copper (II) complexes. Chemistry letters. 2005 Feb;34(2):244-5. https://doi.org/10.1246/cl.2005.244

[5] Salavati-Niasari M, Davar F. In situ one-pot template synthesis (IOPTS) and characterization of copper (II) complexes of 14-membered hexaaza macrocyclic ligand "3, 10-dialkyl-dibenzo-1, 3, 5, 8, 10, 12-hexaazacyclotetradecane". Inorganic Chemistry Communications. 2006 Feb 1;9(2):175-9.

[6] Nazar, S., et al., Rheological properties of cementitious composites with and without nano-materials: A comprehensive review. Journal of Cleaner Production, 2020. 272: p. 122701. https://doi.org/10.1016/j.jclepro.2020.122701

[7] Norhasri MM, Hamidah MS, Fadzil AM. Applications of using nano material in concrete: A review. Construction and Building Materials. 2017 Feb 15; 133:91-7. https://doi.org/10.1016/j.conbuildmat.2016.12.005

[8] Morsy MS, Alsayed SH, Aqel M. Hybrid effect of carbon nanotube and nano-clay on physico-mechanical properties of cement mortar. Construction and Building Materials. 2011 Jan 1;25(1):145-9. https://doi.org/10.1016/j.conbuildmat.2010.06.046

[9] Bautista-Gutierrez KP, Herrera-May AL, Santamaría-López JM, Honorato-Moreno A, Zamora-Castro SA. Recent progress in nanomaterials for modern concrete infrastructure: Advantages and challenges. Materials. 2019 Oct 29;12(21):3548. https://doi.org/10.3390/ma12213548

[10] Muzenski S, Flores-Vivian I, Sobolev K. Ultra-high strength cement-based composites designed with aluminum oxide nano-fibers. Construction and Building Materials. 2019 Sep 30; 220:177-86. https://doi.org/10.1016/j.conbuildmat.2019.05.175

[11] Piro NS, Mohammed AS, Hamad SM. Multiple analytical models to evaluate the impact of carbon nanotubes on the electrical resistivity and compressive strength of the cement paste. Sustainability. 2021 Nov 13;13(22):12544. https://doi.org/10.3390/su132212544

[12] Mutuk H, Mutuk T, Gümüş H, Mesci Oktay B. Shielding behaviors and analysis of mechanical treatment of cements containing nanosized powders. Acta Physica Polonica A. 2016 Jul;130(1):172-4. https://doi.org/10.12693/APhysPolA.130.172
[13] Hamead AA, Ahmed SS, Azzat SR, Abed MS, Hammod GK. Employing recycling materials for the fabrication of smart mortar. Materials Today: Proceedings. 2020 Jan 1; 20:397-402. https://doi.org/10.1016/j.matpr.2019.09.154
[14] Teixeira ED, Pasquini D, Curvelo AA, Corradini E, Belgacem MN, Dufresne A. Cassava bagasse cellulose nanofibrils reinforced thermoplastic cassava starch. Carbohydrate polymers. 2009 Oct 15;78(3):422-31. https://doi.org/10.1016/j.carbpol.2009.04.034
[15] Azeredo HM, Mattoso LH, Wood D, Williams TG, Avena-Bustillos RJ, McHugh TH. Nanocomposite edible films from mango puree reinforced with cellulose nanofibers. Journal of food science. 2009 Jun;74(5): N31-5. https://doi.org/10.1111/j.1750-3841.2009.01186.x
[16] Ali AH, Ibrahim SI, Gharkan MR, Salih WM. Some mechanical and physical properties of cement mortar reinforced by steel wires of scrap tires. Zanco Journal of Pure and Applied Sciences. 2019;31(3):47-51. https://doi.org/10.21271/ZJPAS.31.s3.7
[17] Llanos JH, Tadini CC. Preparation and characterization of bio-nanocomposite films based on cassava starch or chitosan, reinforced with montmorillonite or bamboo nanofibers. International journal of biological macromolecules. 2018 Feb 1; 107:371-82.
[18] Ilyas RA, Sapuan SM, Ishak MR, Zainudin ES. Sugar palm nanofibrillated cellulose (Arenga pinnata (Wurmb.) Merr): Effect of cycles on their yield, physic-chemical, morphological and thermal behavior. International Journal of Biological Macromolecules. 2019 Feb 15; 123:379-88. https://doi.org/10.1016/j.ijbiomac.2018.11.124
[19] Khatib J, Ramadan R, Ghanem H, Elkordi A. Effect of adding phragmites-australis fiber on the mechanical properties and volume stability of mortar. Fibers. 2024 Jan 30;12(2):14. https://doi.org/10.3390/fib12020014
[20] Saleem MH, Abdul-Hamead AA, Othman FM. Performance of waste materials and carbon nanotube in concrete incorporated with carbon fiber. InAIP Conference Proceedings 2022 Aug 17 (Vol. 2437, No. 1). AIP Publishing.
[21] Carrillo-Varela I, Pereira M, Mendonça RT. Determination of polymorphic changes in cellulose from Eucalyptus spp. fibres after alkalization. Cellulose. 2018 Dec; 25:6831-45. https://doi.org/10.1007/s10570-018-2060-4
[22] Sreekala MS, Kumaran MG, Joseph S, Jacob M, Thomas S. Oil palm fibre reinforced phenol formaldehyde composites: influence of fibre surface modifications on the mechanical performance. Applied composite materials. 2000 Nov; 7:295-329. https://doi.org/10.1023/A:1026534006291
[23] Li X, Tabil LG, Panigrahi S. Chemical treatments of natural fiber for use in natural fiber-reinforced composites: a review. Journal of Polymers and the Environment. 2007 Jan; 15:25-33. https://doi.org/10.1007/s10924-006-0042-3
[24] Rong MZ, Zhang MQ, Liu Y, Yang GC, Zeng HM. The effect of fiber treatment on the mechanical properties of unidirectional sisal-reinforced epoxy composites. Composites Science and technology. 2001 Aug 1;61(10):1437-47. https://doi.org/10.1016/S0266-3538(01)00046-X
[25] Ronald Aseer J, Sankaranarayanasamy K, Jayabalan P, Natarajan R, Priya Dasan K. Morphological, physical, and thermal properties of chemically treated banana fiber. Journal of Natural Fibers. 2013 Oct 2;10(4):365-80. https://doi.org/10.1080/15440478.2013.824848
[26] Bledzki AK, Mamun AA, Lucka-Gabor M, Gutowski VS. The effects of acetylation on properties of flax fibre and its polypropylene composites. Express polymer letters. 2008 Jun 1;2(6):413-22. https://doi.org/10.3144/expresspolymlett.2008.50
[27] Senthilkumar K, Rajini N, Saba N, Chandrasekar M, Jawaid M, Siengchin S. Effect of alkali treatment on mechanical and morphological properties of pineapple leaf fibre/polyester composites. Journal of Polymers and the Environment. 2019 Jun 15; 27:1191-201. https://doi.org/10.1007/s10924-019-01418-x
[28] Kanakaraj P, Shaikh B, Karthika K, Yuns M. Scope and Effect of Retting Treatment on Tensile Characteristics of Natural Fiber Extracted from Phragmites Australis (Naanal). Journal of Textile and Apparel, Technology and Management. 2016 Apr 28;10(1).
[29] Yue Y, Han J, Han G, Zhang Q, French AD, Wu Q. Characterization of cellulose I/II hybrid fibers isolated from energycane bagasse during the delignification process: morphology, crystallinity and percentage estimation. Carbohydrate Polymers. 2015 Nov 20; 133:438-47. https://doi.org/10.1016/j.carbpol.2015.07.058
[30] Tiwari YM, Sarangi SK. Characterization of raw and alkali treated cellulosic Grewia Flavescens natural fiber. International Journal of Biological Macromolecules. 2022 Jun 1; 209:1933-42. https://doi.org/10.1016/j.ijbiomac.2022.04.169
[31] Nwa-David CD. Performance of potato starch admixture on fresh and hardened behaviours of concrete at varied mix design ratios. Engineering and Technology Journal. 2024;42(05):540-7. https://doi.org/10.30684/etj.2024.145272.1654

[32] Revathy R, Sajini T, Augustine C, Joseph N. Iron-based magnetic nanomaterials: sustainable approaches of synthesis and applications. Results in Engineering. 2023 Jun 1; 18:101114. https://doi.org/10.1016/j.rineng.2023.101114
[33] Nazari A, Riahi S, Riahi S, Shamekhi SF, Khademno A. Influence of Al2O3 nanoparticles on the compressive strength and workability of blended concrete. Journal of American Science. 2010;6(5):6-9.
[34] Dahesh AZ, Othman FM, Abdul-Hamead AA. Improve mass concrete by controlling the crack sealing mechanism using microcapsules of zinc oxide. InMaterials Science Forum 2020 Aug 14 (Vol. 1002, pp. 541-550). Trans Tech Publications Ltd.
[35] Nwa-David CD. Performance of potato starch admixture on fresh and hardened behaviours of concrete at varied mix design ratios. Engineering and Technology Journal. 2024;42(05):540-7. https://doi.org/10.30684/etj.2024.145272.1654
[36] French AD. Idealized powder diffraction patterns for cellulose polymorphs. Cellulose. 2014 Apr;21(2):885-96. https://doi.org/10.1007/s10570-013-0030-4
[37] Chen HongYan CH, Liu JinBao LJ, Chang Xing CX, Chen DaMing CD, Xue Yuan XY, Liu Ping LP, Lin HuaLin LH, Han Sheng HS. A review on the pretreatment of lignocellulose for high-value chemicals.
[38] Venugopal A, Boominathan SK. Physico-chemical, thermal and tensile properties of alkali-treated acacia concinna fiber. Journal of Natural Fibers. 2022 Aug 3;19(8):3093-108. https://doi.org/10.1080/15440478.2020.1838998
[39] Chen H, Wu J, Shi J, Zhang W, Wang H. Effect of alkali treatment on microstructure and thermal stability of parenchyma cell compared with bamboo fiber. Industrial Crops and Products. 2021 Jun 1; 164:113380.
[40] Wu HF, Shen JJ, Liu Y, Hu YY. Effect of nano-Al2O3 on the mechanical and microstructural properties of cement-based grouting material. Case Studies in Construction Materials. 2024 Dec 1;21: e03846. https://doi.org/10.1016/j.cscm.2024.e03846
[41] Barbhuiya S, Das BB, Kanavaris F. Biochar-concrete: A comprehensive review of properties, production and sustainability. Case Studies in Construction Materials. 2024 Jul 1;20: e02859. https://doi.org/10.1016/j.cscm.2024.e02859
[42] Mehta A, Siddique R. Properties of low-calcium fly ash based geopolymer concrete incorporating OPC as partial replacement of fly ash. Construction and building materials. 2017 Sep 30; 150:792-807. https://doi.org/10.1016/j.conbuildmat.2017.06.067
[43] Zhang P, Wang L, Wei H, Wang J. A critical review on effect of nanomaterials on workability and mechanical properties of high-performance concrete. Advances in Civil Engineering. 2021;2021(1):8827124. https://doi.org/10.1155/2021/8827124
[44] Hussein T, Kurda R, Mosaberpanah M, Alyousef R. A review of the combined effect of fibers and nano materials on the technical performance of mortar and concrete. Sustainability. 2022 Mar 16;14(6):3464.
[45] Su DY, Pang JY, Huang XW. Mechanical and Dynamic Properties of Hybrid Fiber Reinforced Fly-Ash Concrete. Advances in Civil Engineering. 2021;2021(1):3145936. https://doi.org/10.1155/2021/3145936
[46] Gholampour A, Danish A, Ozbakkaloglu T, Yeon JH, Gencel O. Mechanical and durability properties of natural fiber-reinforced geopolymers containing lead smelter slag and waste glass sand. Construction and Building Materials. 2022 Oct 17; 352:129043. https://doi.org/10.1016/j.conbuildmat.2022.129043
[47] Ahmed W, Lim CW. Production of sustainable and structural fiber reinforced recycled aggregate concrete with improved fracture properties: A review. Journal of Cleaner Production. 2021 Jan 10; 279:123832. https://doi.org/10.1016/j.jclepro.2020.123832